

Buck Converter Control for Lead Acid Battery Charger using Peak Current Mode

Asep Nugroho¹, Estiko Rijanto², Latif Rozaqi³

Research Center for Electrical Power and Mechatronics, Indonesian Institute of Sciences, Bandung, Indonesia

Article Info

Article history:

Received Feb 4, 2017

Revised Apr 4, 2017

Accepted Apr 18, 2017

Keyword:

Buck converter

Charger

Control

Lead acid battery

Peak current mode

ABSTRACT

DC-DC buck converters are used for battery chargers in many applications including renewable energy sources, inverters, electric vehicles and robots. In this paper a buck converter was built and its controller was developed using peak current control mode for current loop and phase lag for voltage loop. This paper proposes a formulation of plant disturbance due to load variation to obtain a nominal model based on small signal approach. The controller was derived analytically based on the nominal model. Experiment results show that the buck control system functions well in regulating the output voltage. During the start up without any load it can reduce input voltage from 300 V to output voltage of 133.9 V in 19.3 ms. The developed controller can maintain the output voltage under load variation from no load to sudden load of 0.26 A. When it was implemented to charge a lead acid battery string, constant current of 3.36 A was charged in the first 173 minutes followed by constant voltage of 134.7 V until the end of charging at time 483 minutes. Thus, the developed control system of lead acid battery charger works well.

Copyright © 2017 Institute of Advanced Engineering and Science.
All rights reserved.

Corresponding Author:

Asep Nugroho,

Research Center for Electrical Power and Mechatronics,

Indonesian Institute of Sciences (LIPI),

Komplek LIPI Gd. 20, Jl. Cisitua Sangkuriang 21/154D, Bandung, Indonesia.

Tel: +62-22-2503055

Email: asepnugroho.lipi@gmail.com

1. INTRODUCTION

Despite of low energy density, lead acid batteries are still commonly used for energy storage, emergency power back up, engine ignition, vehicle lighting, and generator starting due to their low cost and easy of availability. In off grid PV application, lead acid battery has less benefit cost ratio and simple net present value compared to lithium-ion battery [1] However, lead acid battery requires high maintenance to keep it at certain appropriate capacity. The failure to fully recharge the battery may cause plate sulfation which in turn reduces cell capacity. Conversely, higher charge current may increase hydrogen gas generation and heat as well as accelerates the positive plate corrosion and shortens the life of the battery. Lead acid battery manufacturers classify their own charging methods [2] [3]. Charging methods are dependent on battery applications including main power source applications and stand-by/back-up power applications [2]. Standard charging which incorporates constant current followed by constant voltage as well as rapid charging which incorporates constant current followed by two steps constant voltage are used for main power source applications [2]. While trickle charging and float charging are used for stand-by power applications [2]. A smart charger supplies constant current to initially charge the battery, then it automatically switches to a constant voltage mode to float charge or maintain the battery [3]. A smart charger also monitors the battery's state of charge (SOC) and will automatically start charging when the battery falls below a specific voltage [3].

In photovoltaic applications some charging methods have been proposed by many researchers in order to keep the battery in higher SOC within shorter time when the output energy of solar cell is sufficient [4]-[5]. The charging current and battery voltage are continuously monitored. First the battery is charged within maximum charge rate until the voltage reaches predefined maximum limit voltage. Then in the second stage the battery is charged again within maximum charge rate which is lower than the first charge stage. Every time its voltage reaches the predefined maximum limit voltage the charge rate is reduced until its predefined minimum charge rate which indicates 100% of SOC [4]. A method called decreased charging current based on SOC enhances the above method by combining the maximum limit voltage and SOC estimated using a suitable model to determine the charging rate of each stage [5]. Concerning battery modeling, results of experimental study revealed that Lead acid battery model named CIEMAT Copetti model can express well the characteristics of Lead acid battery [6]. Impact of charging process on Lead acid battery and the behaviour of different internal parameters of the battery was simulated using CIEMAT model [7].

Sliding mode control (SMC) has been used to control dc-dc buck converters [8]-[9]. The sliding mode controller was proved to be effective through numerical simulation of a dc-dc buck converter having input voltage of 20V and nominal capacity of around 2.5W [8]. A dynamical model of dc-dc buck converter with SMC by using generalized state space averaging was proposed and proved to effectively represent switching model in less computational time through numerical simulation [9]. A battery charger was proposed using topology of full bridge DC-DC converter connected in series with SEPIC converter for power factor correction [10]. They explain the topology and experiment results but they did not describe about controller design in detail [10].

In this paper, a prototype of battery charger is built and its controller is developed. The battery charger uses a buck dc-dc converter topology which minimizes the use of components. The converter is to convert a DC voltage source of 280 V to 325 V into a voltage level suitable for charging a series of lead acid batteries having terminal voltage of 120 V. To realize such a converter, a power electronic circuit is built using appropriately selected inductor, capacitor, MOSFET and other components. Then a controller is designed to properly charge the battery. To design a controller, firstly small signal dynamical model is derived. The controller is composed of two control loops those are current control loop and voltage control loop. The current controller is designed using peak current mode controller while the voltage controller is designed using proportional integral (PI) action. This paper proposes a formulation of nominal plant and plant disturbance based on load variation. The PI controller is analytically designed based on the nominal plant. Finally, the controller was implemented to the converter through experiment.

Section 2 of this paper presents conceptual design, specification and dynamical modeling of the buck DC-DC converter. Section 3 is devoted to controller design of the buck DC-DC converter using the derived dynamical model. Section 4 describes experiment results and discussion. Section 5 summarizes the conclusions.

2. RESEARCH METHOD

2.1. Modeling of the Buck DC-DC Converter

Figure 1 shows block diagram of the buck DC-DC converter control system developed in this paper. This control system consists of a buck DC-DC converter and its controller. The buck converter is constructed by inductor L, diode D1, capacitor C, and switch SW1 which is equipped with its driver circuit.

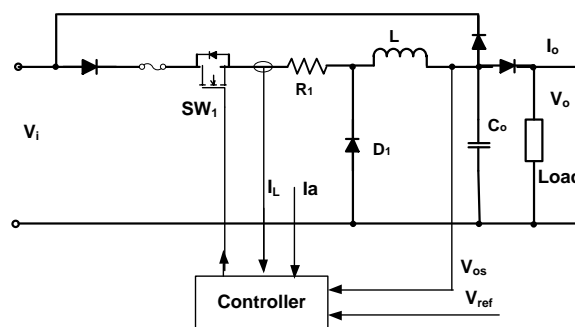


Figure 1. The developed DC-DC buck converter control system

The buck converter operates in two switching modes those are closed mode (switch on) and open mode (switch off). The dynamics of the converter is governed by the following switched model dynamical equations.

$$L \frac{di_L(t)}{dt} = -V_o(t) + uV_i \quad (1)$$

$$C \frac{dV_o(t)}{dt} = -\frac{V_o(t)}{R} + i_L(t) \quad (2)$$

where u denotes the switch status. The status $u = 1$ represents the closed mode while $u = 0$ represses the open mode. From the dynamics equations in (1) - (2) the following average small signal model can be derived.

$$\begin{bmatrix} \dot{x}_1 \\ \dot{x}_2 \end{bmatrix} = \begin{bmatrix} 0 & \frac{-1}{L} \\ \frac{1}{C} & \frac{-1}{RC} \end{bmatrix} \begin{bmatrix} x_1 \\ x_2 \end{bmatrix} + \begin{bmatrix} \frac{V_{in}}{L} \\ 0 \end{bmatrix} \hat{d} + \begin{bmatrix} \frac{Dn}{L} \\ 0 \end{bmatrix} \hat{v}_i \quad (3)$$

where x_1 is small deviation of current value around its nominal value and x_2 is small deviation of output voltage value around its nominal value. \hat{d} and \hat{v}_i represent deviation of duty ratio around nominal value and the deviation of input voltage value around its nominal value, respectively.

It is assumed that the deviation of the load can be represented by the deviation of load resistance. Therefore, the following relationships can be formulated.

$$\frac{1}{RC} = \frac{1}{C(R_n + \Delta R)} = \frac{1}{CR_n} \pm \delta \quad (4)$$

$$R_n = \frac{2(R_1 R_2)}{(R_1 + R_2)} \quad (5)$$

$$\delta \leq \frac{1}{C} \frac{(R_2 - R_1)}{2(R_1 R_2)} \quad (6)$$

R_n is nominal value of the load resistance, while R_1 and R_2 are given values from the minimum and maximum load selected. By substituting (4) and (6) into (3) the following state space equation is obtained.

$$\dot{x} = A\hat{x} + B_1\hat{d} + B_2\hat{v}_i + B_3f_d(\delta, \hat{x}) \quad (7)$$

$$A = \begin{bmatrix} 0 & \frac{-1}{L} \\ \frac{1}{C} & \frac{-1}{CR_n} \end{bmatrix}; B_1 = \begin{bmatrix} \frac{V_{in}}{L} \\ 0 \end{bmatrix}; \left. \begin{array}{l} B_2 = \begin{bmatrix} \frac{Dn}{L} \\ 0 \end{bmatrix}; B_3 = \begin{bmatrix} 0 \\ 1 \end{bmatrix} \end{array} \right\} \quad (8)$$

$$f_d(\delta, \hat{x}) = \delta\hat{x}_2 \quad (9)$$

From (7) it is obvious that effect of input voltage variation can be considered as external disturbance with the input matrix B_2 while effect of load variation can be handled as an internal disturbance represented by $f_d(\delta, \hat{x})$.

2.2. Specification of the Buck DC-DC Converter

Table 1 shows the design specification of the buck DC-DC converter.

Table 1. Specification of the Buck DC-DC Converter

Parameter	Value	Unit
Maximum power, Pmax	1200	W
Maximum input voltage, Vimax	328	V
Minimum input voltage, Vimin	280	V
Nominal input voltage, Vin	308	V
Reference output voltage, Vref	132	V
Switching frequency, fs	36000	Hz

From Table 1, values of nominal duty ratio D_n , minimum duty ratio D_{min} and maximum duty ratio D_{max} are $D_n = 0.43$, $D_{min} = 0.4$, and $D_{max} = 0.47$. The minimum output current and the maximum output current are set to be $I_{omin} = 0.87A$, and $I_{omax} = 9A$. The current ripple is 1.74 A and the output voltage ripple is 0.23 V. Furthermore, the values of load resistances are $R_1 = 14.67 \text{ Ohm}$, $R_2 = 151.95 \text{ Ohm}$, and $R_n = 26.76 \text{ Ohm}$.

3. CONTROLLER DESIGN

From the state space Equation in (7) the following transfer functions can be obtained.

$$\hat{x}_1(s) = \frac{(R_n C s + 1) \left(\frac{V_{in} \hat{d} + D_n \hat{v}_i}{R_n} - C f_d \right)}{(LC)s^2 + \frac{L}{R_n} s + 1} \left. \vphantom{\hat{x}_1(s)} \right\} \quad (10)$$

$$= G_{id}(s) \hat{d} + G_{ig} \hat{v}_i + G_{ifd} f_d$$

$$\hat{x}_2(s) = \frac{v_{in} \hat{d} + D_n \hat{v}_i + s f_d}{(LC)s^2 + \frac{L}{R_n} s + 1} \left. \vphantom{\hat{x}_2(s)} \right\} \quad (11)$$

$$= G_{vd}(s) \hat{d} + G_{vg} \hat{v}_i + G_{vfd} f_d$$

Peak current mode controller has many advantages over duty-ratio controller such as better line noise rejection, automatic overload protection, and especially design flexibility in improving small-signal dynamics [12]. A large number of small-signal models of peak current modulator have been proposed, for example [11]-[12]. The previous models give accurate expressions for the control-to-output transfer function and the output impedance but not for the audio susceptibility so the improved models have been proposed [13]-[14]. By adopting the previous results of other researchers, the peak current modulator can be modeled as follows.

$$\hat{d} = F_m \{ \hat{i}_c - \hat{x}_1 - F_g \hat{v}_i - F_v \hat{x}_2 \} \quad (12)$$

$$F_m = \frac{1}{M_a T_s}; F_g = \frac{D^2 T_s}{2L}; F_v = \frac{(1-2D)T_s}{2L} \quad (13)$$

M_a is rate of additional external current ramp in A/sec. From (10), (11) and (12) the following control-to-output voltage transfer function can be derived.

$$G_{vc}(s) = \frac{\hat{x}_2(s)}{\hat{i}_c(s)} \Big|_{\hat{v}_i(s)} = \frac{G_{co}}{\left(\frac{s}{\omega_c}\right)^2 + \frac{s}{Q_c \omega_c} + 1} \quad (14)$$

Substituting parameter values of the buck DC-DC converter the values of the peak current mode controller parameters can be obtained as listed in Table 2.

Table 2. Example of peak current mode controller parameter values

Parameter	Value
F_m	34.42
F_g	0.002
F_v	0.0016
G_{co}	25.61
ω_c	106.877,23
Q_c	0.01

Thus the following transfer function is obtained.

$$G_{vc}(s) = \frac{2,9 \times 10^{11}}{s^2 + 8,5 \times 10^6 s + 1,1 \times 10^{10}} \quad (15)$$

A voltage controller is designed based on equation (15). Voltage loop is closed using the voltage controller as shown in Figure 2.

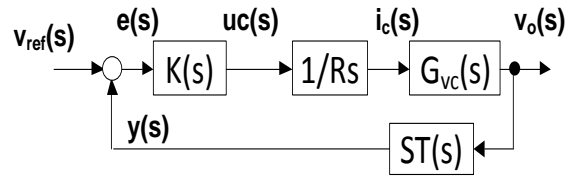


Figure 2. The designed voltage control loop

An augmented voltage controller is composed by $K(s)$ and $\frac{1}{R_s}$ where R_s denotes current sensor gain. The controller is designed so that the converter output voltage $v_o(s)$ follows the given reference $v_{ore}(s)$. The voltage controller receives voltage feedback signal $y(s)$ from the voltage sensor $ST(s)$. The voltage controller produces current command signal $i_c(s)$ to the peak current control loop $G_{vc}(s)$. In this paper, the voltage controller is designed using proportional and integral actions as Equation 16. This voltage controller is equipped with a low pass filter to filter out noise due to high frequency switching.

$$K_1(s) = \left[K_p + \frac{K_i}{s} \right] \left[\frac{1}{\frac{1}{\omega_p}s + 1} \right] \quad (16)$$

By setting cross over frequency value ω_c and phase angle margin value α , the voltage controller parameter values can be calculated using unity gain and phase angle margin.

4. IMPLEMENTATION RESULTS AND DISCUSSION

Figure 3 shows the experiment set up consisting of a Lead Acid batteries string and the developed charger using buck DC-DC converter topology. The controller is realized using analog and digital circuits. In order to verify the effectiveness of the developed control system some experiments have been conducted. First experiments without load and with a resistive load were carried out using input voltage of 300 V. Then the charger was applied to 10 Lead Acied batteries connected in serial. Each battery has the capacity of 45Ah.



(a) Lead Acid battery string



(b) The developed research prototype of charger

Figure 3. The developed prototype of LA battery charger

Figures 4 to 8 show experiment results without any load and with a resistive load. Figure 4 shows the experimental result when the charger is started up without any load while Figure 5 when the load was

suddenly added under steady state condition. The horizontal axis indicates time in second and the vertical axis is voltage in Volt. The blue line represents output voltage while the red line expresses output current. For measurement purpose, the gains of blue line voltage and red line current sensors are $\frac{2,86}{133}$ [V/V] and $\frac{5,03}{2,6}$ [V/A], respectively. From Figure 4 it can be noted that the output voltage rises smoothly from 0 V to the steady state value of 133.9 V with settling time around 19.3 ms. The output current keeps constant during transient phase. In Figure 5 the output voltage is kept constant while the output current raises from 0 A to 0.26 A.

Figure 6 shows the output signal of voltage controller ($u_c(t)$) and current feedback signal ($v_{iL}(t)$) during start up without load, while Figure 7 shows the same signals under loading. These figures demonstrate the performances of the peak current control loop. It can be noted that the peak value of $v_{iL}(t)$ is always less than the value of $u_c(t)$ which demonstrates that the peak current controller works well. Their relationship may be expressed as $v_{iL_peak}(t) \leq a_1 u_c(t) - a_2$ where v_{iL_peak}, a_1, a_2 are all positive values. Figure 8 shows current command signal $u_c(t)$ and PWM output signal. Note that duty ratio of PWM output signal varies according to the value of $u_c(t)$.

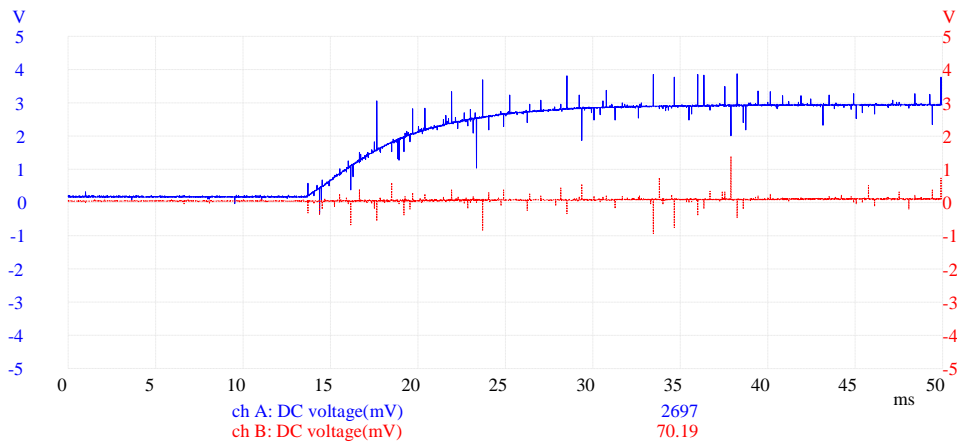


Figure 4. Output voltage (blue) and output current (red) during start up without load

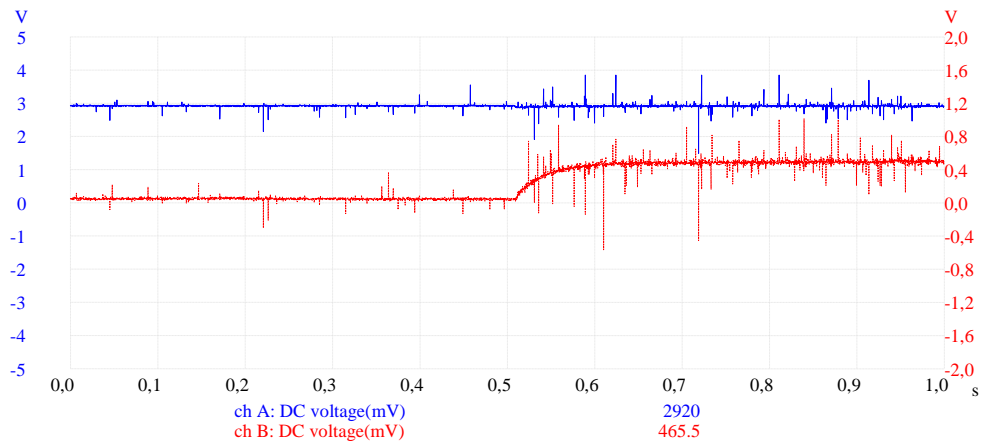


Figure 5. Output voltage (blue) and output current (red) under suddenly added resistive load (1R)

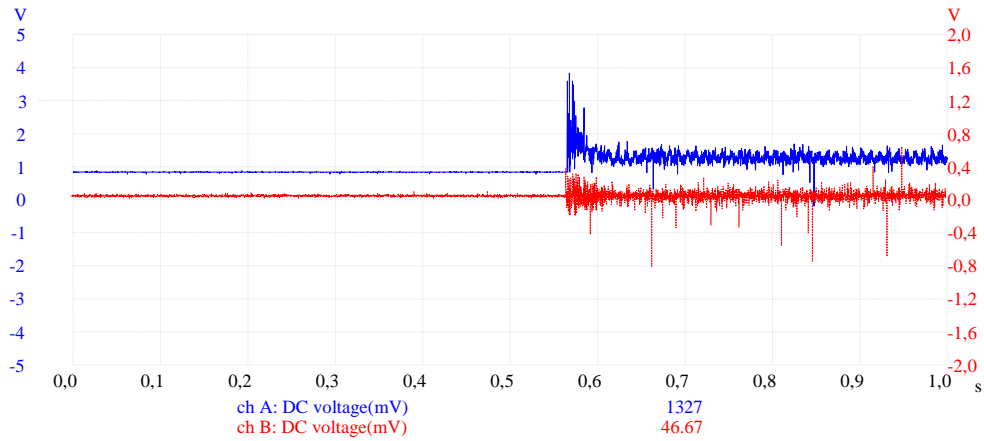


Figure 6. Internal voltage controller output (blue) (= current command) and current feedback (red) during start up without load

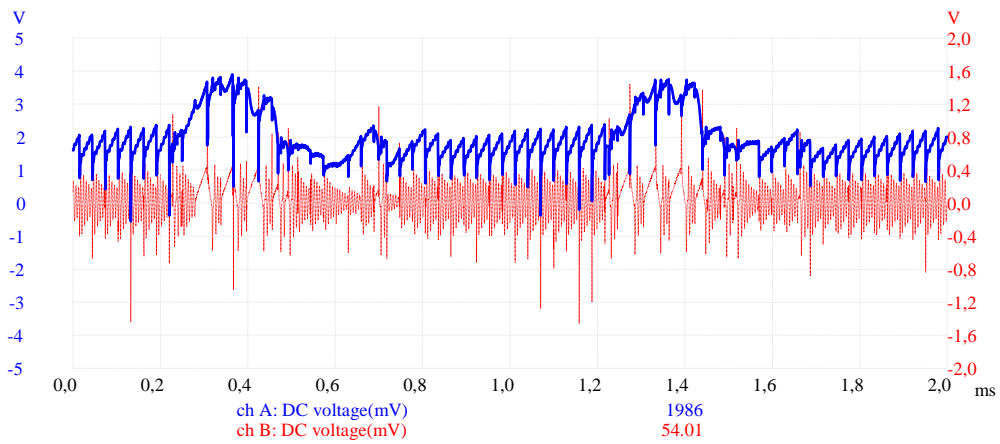


Figure 7. Current command (blue) and current feedback (red) under resistive load (1 R)

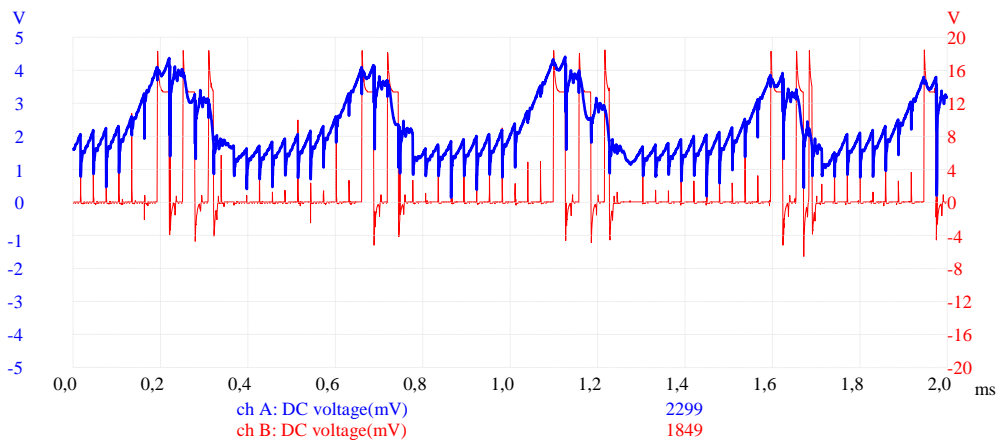


Figure 8. Current command (blue) and PWM output (red) under resistive load (1 R)

Next, the developed DC-DC buck converter was implemented to charge the Lead Acid batteries. The output voltage reference value was set to 135.1 V and the initial battery voltage was 123.3 V. During experiment, at the beginning the sampling time was varied due to rapid change in the battery voltage. After 8 minutes since the experiment started the sampling time was set constant at 5 minute. Figures 9 to 10 show the experimental results. Figure 9 shows the output voltage during battery charging. From time 0 to 8 minutes the output voltage rises rapidly from 123.3 V to 129.4 V. In 173 minutes the output voltage reached 134.5 V. At time 238 minutes the output voltage became 134.7 V. Until the end of experiment at time 483 minutes the output voltage was kept almost constant at the average value of 134.72 V. Figure 10 shows the corresponding output current. From time 0 to 173 minutes the output current was almost constant at the average value of 3.36A. After that the current decreases until 0.7 A at time 483 minutes.

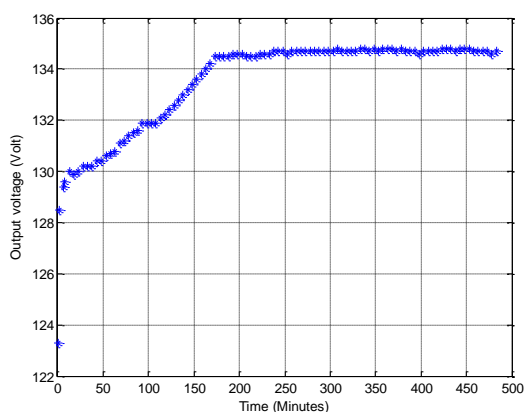


Figure 9. Output voltage during battery charging

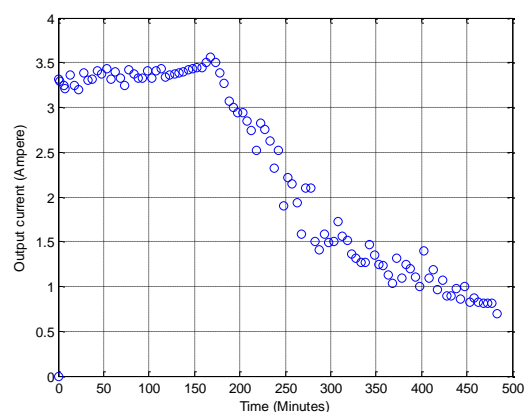


Figure 10. Output current during battery charging

These experimental results may be analyzed using Lead acid battery model [6]-[7]. When approaching the full State of Charge (SOC), internal resistance and temperature increase rapidly. This phenomena leads to the decreasing rate of change of the voltage.

5. CONCLUSION

From the experimental results the following conclusion can be drawn. During the start up without any load the output voltage of the developed buck DC-DC converter rises smoothly from 0 V to the steady state value of 133.9 V. When it is suddenly loaded the output voltage is well regulated while the output current rises smoothly. The output current is always less than the current command which proves that the peak current control works well. The prototype worked well when it was used to charge a LA battery string whose capacity is 45Ah. It worked with charging strategy of constant current constant voltage bringing the battery terminal voltage from 123.3 V to 134.72 V in total charging time of 483 minutes.

ACKNOWLEDGEMENTS

The authors thank to Ganjar Ari Priyatno who has helped in designing and developing the prototype as well as conducting the experiment.

REFERENCES

- [1] S. Anuphapharadorn, S. Sukchai, C. Sirisamphanwong, and N. Ketjoy, "Comparison the Economic Analysis of the Battery between Lithium-ion and Lead-acid in PV Stand-alone Application," *Energy Procedia*, vol. 56, no. C, pp. 352–358, 2014.
- [2] Matsushita Battery Industrial Co.Ltd., "Panasonic Sealed Lead-Acid Batteries Technical Handbook 2000," pp.1-77, January 2000.
- [3] Yuasa, "Technical Manual Powersports Batteries," 2901 Montrose Avenue, Laureldale, PA 19605-2752, yuasabatteries.com, 2014.
- [4] E. Koutroulis and K. Kalaitzakis, "Novel battery charging regulation system for photovoltaic applications," *IEEE Proc. - Electr. Power Appl.*, vol. 151, no. 2, p. 191, 2004.
- [5] T. Wu, Q. Xiao, L. Wu, J. Zhang, and M. Wang, "Study and Implementation on Batteries Charging Method of

- Micro-Grid Photovoltaic Systems,” *Smart Grid Renew. Energy*, vol. 02, no. 04, pp. 324–329, 2011.
- [6] N. Achaibou, M. Haddadi, and A. Malek, “Modeling of Lead Acid Batteries in PV Systems,” *Energy Procedia*, vol. 18, pp. 538–544, 2012.
- [7] A. Selmani, A. Ed-Dahhak, M. Outanoute, A. Lachhab, M. Guerbaoui, and B. Bouchikhi, “Performance Evaluation of Modelling and Simulation of Lead Acid Batteries for Photovoltaic Applications,” *Int. J. Power Electron. Drive Syst.*, vol. 7, no. 2, p. 472, Jun. 2016.
- [8] H. Guldemir, “Study of Sliding Mode Control of DC-DC Buck Converter,” *Energy Power Eng.*, vol. 03, no. 04, pp. 401–406, 2011.
- [9] S. Chonsatidjamroen, “Dynamic Model of a Buck Converter with a Sliding Mode Control,” vol. 5, no. 12, pp. 386–391, 2011.
- [10] M. Z. Efendi, N. A. Windarko, and M. F. Amir, “Design and Implementation of Battery Charger with Power Factor Correction using Sepic Converter and Full-bridge DC-DC Converter,” *J. Mechatronics, Electr. Power, Veh. Technol.*, vol. 4, no. 2, p. 75, Dec. 2013.
- [11] F. D. Tan and R. D. Middlebrook, “A unified model for current-programmed converters,” *IEEE Trans. Power Electron.*, vol. 10, no. 4, pp. 397–408, Jul. 1995.
- [12] R. B. Ridley, “A new, continuous-time model for current-mode control (power convertors),” *IEEE Trans. Power Electron.*, vol. 6, no. 2, pp. 271–280, Apr. 1991.
- [13] B. Johansson, “Improved Models for DC-DC Converters,” ISBN 91-88934-29-2, *Licentiate Thesis, Lund University, Lund Sweden, 2003*.
- [14] B. Johansson, “DC-DC Converters - Dynamic Model Design and Experimental Verification,” ISBN 91-88934-34-9, *Doctoral Dissertation, Lund University, Lund Sweden, 2004*.

BIOGRAPHIES OF AUTHORS



Asep Nugroho was born in Bantul-Yogyakarta, Indonesia in 1987. He received Bachelor degree from Gadjah Mada University in Electronic and Instrumentation in 2011 and completed Master degree in same univeristy in 2015. His research interests was on DC/DC converter, modelling control system, charging system, battery management system and control algorithm. He currently works as an junior researcher in Indonesian Institute of Sciences (LIPI) to develop DC/DC converter and battery management systems for Li-ion batteries.



Estiko Rijanto was born in Purbalingga – Central Java, Indonesia in 1967. He enrolled at ITB (Indonesia) in 1987, later he moved to Japan in 1988 and completed his B.Eng. degree at Tokyo University of Agriculture and Technology (TUAT), in 1993. He recieved the M.Eng. and Dr.Eng. degrees from TUAT in 1995 and 1998, respectively. He took post doctoral programs at VBL Tokyo where he completed his book on Robust Control: Theory for Application, and at industry in Maebashi where he envolved in R&D of EPS. Since 2002 he has been conducting R&D at the Indonesian Institute of Sciences (LIPI). Presently he is a Professor Research on Applied Control at LIPI. His research interests are in control system and its applications for mechatronics, electrical power, power electronics and bio-chemical processes.



Latif Rozaqi was born in Temanggung-Central Java, Indonesia in 1989. He received bachelor degree from Diponegoro University in Mechanical Engineering 2013. His research interests was on charging system, battery management system and control algorithm. He currently works as an junior researcher in Indonesian Institute of Sciences (LIPI) to develop charging and battery management systems for Li-ion batteries.